

Comparative Study of Various Algorithms on Hyperspectral Data

¹ Payas Deshpande, ¹Manas Rode, ¹Meet Raychura, ¹Sridhar S., ¹Dr. K. Nandhini, ²Dr. Shilpa Gite

Submitted: 24/10/2023

Revised: 16/12/2023

Accepted: 26/12/2023

Abstract: Hyperspectral remote sensing data, captured across a broad spectrum, provides rich information for various applications, which is including land cover classification and the environmental monitoring. In this research paper, we conduct a comprehensive comparative study of machine learning and deep learning algorithms on three widely used hyperspectral datasets: Indian Pines, Pavia University, and Salinas. For machine learning, Support Vector Classification (SVC) and Random Forest algorithms were selected due to their proven effectiveness in classification tasks. Additionally, we explored deep learning techniques by implementing 1D CNN and 2D CNN models, leveraging the spatial and spectral characteristics inherent in hyperspectral data. Our experimental results reveal that among the machine learning algorithms, Random Forest demonstrated competitive performance, while SVC exhibited commendable accuracy. However, the deep learning models, particularly the 2D CNN architecture, outperformed the traditional machine learning algorithms, achieving an impressive accuracy of 98%. This outcome highlights the capability of deep learning models, specifically designed to capture spatial patterns in hyperspectral data, to provide superior classification accuracy.

Keywords: *Hyperspectral, Support Vector Classification (SVC), effectiveness, algorithms*

1. Introduction

Remote Sensing and GIS as a field were introduced in the 1960 by Evelyn L. Pruitt, marking the beginning of a renewed interest in Earth observations from space and airborne platforms. The Landsat satellites, operational since 1972, have been pivotal in global research, with sensors like the Multispectral Scanner (MSS), Thematic Mapper (TM), and Enhanced Thematic Mapper Plus (ETM+) contributing high-resolution images for various applications. These technological developments underscore the evolution and expanding utility of remote sensing in contemporary Earth observation efforts[1].

Multispectral and hyperspectral imaging are two distinct approaches in the realm of remote sensing, each offering unique advantages and trade-offs. Multispectral data captures information across a limited number of predefined spectral bands, typically ranging from three to ten bands, providing a broad overview of the scene[2]. In contrast, hyperspectral imaging acquires a much finer spectrum, often consisting of hundreds of contiguous bands, allowing for a more detailed and comprehensive characterization of the observed environment. While multispectral data is advantageous in terms of simplicity, cost-effectiveness, and ease of interpretation, it may lack the specificity required for certain applications that demand a more nuanced spectral analysis. On the other hand, hyperspectral data excels in discerning subtle

spectral differences, offering enhanced discriminatory capabilities, but it comes with increased data complexity, computational demands, and higher costs[3].

The rapid advancement of remote sensing technology[4] has led to the widespread application of hyperspectral images. The precise classification of ground features through hyperspectral images is a significant research focus garnering widespread attention. This paper [5] reviews hyperspectral image classification methods, focusing on supervised, semi-supervised, and unsupervised approaches. Hyperspectral images, acquired with high spatial and spectral resolution, find applications in diverse fields such as environmental monitoring[6], military surveillance[7], agriculture, forestry[8] and medical diagnostics[9]. These images capture detailed spectral information, reflecting the physical and chemical composition of objects, making them valuable for image classification.

In our Research Several hyperspectral datasets have been employed to evaluate and compare the performance of various algorithms. The Indian Pines dataset, originating from Northwestern Indiana, United States, is widely utilized in hyperspectral image analysis. It comprises 224 spectral bands and is commonly employed for tasks such as land cover classification. Additionally, the Pavia University dataset, acquired over Pavia, Italy, is another valuable resource in hyperspectral research, offering high spatial resolution with 103 spectral bands.

Lastly, the Salinas dataset, collected over Salinas Valley, California, features 224 bands and is frequently utilized for applications like agriculture monitoring and land cover classification. These datasets serve as essential

¹Artificial Intelligence and Machine Learning Department, Symbiosis Institute of Technology, Symbiosis International (Deemed University), Pune, India.

² Symbiosis Centre for Applied AI, Symbiosis International (Deemed University), Pune, India.

Corresponding Author: Dr. K. Nandhini

benchmarks, enabling a comprehensive assessment of algorithmic performance across diverse spectral and spatial characteristics[10].

The contribution of our research lies in conducting a comprehensive comparative study of various algorithms applied to hyperspectral data analysis. Through meticulous investigation and evaluation, we aim to provide valuable insights into the strengths and weaknesses of different algorithms in processing

2. Literature Review

hyperspectral datasets. This comparative analysis serves as a guide for researchers and practitioners in choosing the most effective algorithms for specific applications involving hyperspectral data. Our research contributes to advancing the understanding of algorithmic performance in the context of hyperspectral image analysis, thereby facilitating informed decision-making in the selection and implementation of algorithms for diverse hyperspectral data scenarios.

Table 1. Comparison of methods available in the literature

Ref No	Model	Objective	Dataset	Performance	Limitation and future scope
11	Deep CNN	CNN for Hyperspectral Image Classification	Indian Pines data set, the Salinas data set, and the University of Pavia data set	Indian Pines:94.24 Salinas:95.42 Pavia:96.73	Does not provide a comprehensive evaluation
12	DAGCN	Deep Attention Graph Convolutional Network for Hyperspectral Image Classification	Indian Pines data set, the Salinas data set, and the University of Pavia data set	Indian Pines:98.61	Computational complexity is high
13	SFE-SCNN	CNN based on spectral feature enhancement (SFE-SCNN)	Kennedy Space center, Salinas, Indian Pines	Indian Pines:98.72 SA:99.56	Does not compare the proposed method with other
14	hybrid CNN(2D-3D)	Hybrid 3D-2D Convolutional Neural Networks for HIC	Salinas (SA), Pavia University (PU), and Indian pines (IP)	OA:9736 KAPPA:96.70 AA:9766	Does not provide any visualization
15	DFFN	Classification With Deep Feature Fusion Network	Salinas (SA), Pavia University (PU), and Indian pines (IP)	Indian Pines:98.52 Salinas:98.87 Pavia:98.73	Does not provide any analysis of parameters and hyperparameters
16	CNN,	To enhance CNN's generalization performance for HSIC.	Salinas (SA), Pavia University (PU), and Indian pines (IP)	IP=98.94% SA = 99.9876% PU= 99.9070% Hybrid=99.9628%	Usage of L1, L2, Dropoff methods which is unacceptable
17	CNN STN	New method using STN (scaled, translated and rotated) and CNN classifier for HSI classification	SA, Kennedy Space center (KSC)	SA CNN-Dropout = 94.83+1.59 CNN-Dropblock = 95.24+0.50 KSC CNN-Dropout = 96.80+2.50 CNN-Dropblock = 98.85+0.09	Proposed techniques may not work on diverse hyperspectral datasets.

18	CNN (Hybrid Model 3D/2D)	low-complexity 3D-2D CNN model	IP, SA, PU, PAVIA Center, Salina Full Scene, Botswana	SA + SFS = 94.36 IP = 68.32 PU = 94.84 Botswana = 80.23	Requires a huge computation
19	CNN (Hybrid Model 3D/2D)	Hybrid model with 3D to 2D	IP, SA, PU	SA = 99.98 IP = 98.01 PU = 99.20	The model tends to overfit
20	CNN	To create a Fused features to apply CNN	IP, SA, PU	SA = 0.9994 IP = 0.9902 PU = 0.9994	Execution time is high

[21] This paper combines CNNs and RNNs to form a hierarchical convolutional recurrent neural network (HCRNN) that can extract temporal and spatial features from the spectral data of multispectral remote sensing images for pixel-level classification.

[22] This paper proposes a novel backbone network called SpectralFormer that uses transformers to model the sequence attributes of spectral signatures and learn spectrally local sequence information from neighboring bands of hyperspectral images.

[23] This paper provides a comprehensive overview of the deep learning methods for hyperspectral image classification, including the main challenges, the network architectures, the data augmentation techniques, and the evaluation metrics.

[24] This paper combines deep convolutional neural networks (DCNNs) and Markov random fields (MRFs) to perform spectral-spatial classification of hyperspectral images, where the DCNNs can learn the spectral features and the MRFs can model the spatial context.

[25] This paper reviews the recent advances of convolutional neural networks (CNNs) for hyperspectral image classification, and discusses the challenges, the network architectures, the data preprocessing methods, and the future directions.

[26] This paper applies convolutional neural networks (CNNs) to extract deep features from hyperspectral images and use them for classification, and also proposes a spectral-spatial classification strategy based on CNNs and principal component analysis (PCA).

[27] This paper provides a comprehensive study of the deep learning methods for hyperspectral image analysis, covering the topics of data preprocessing, feature extraction, feature fusion, feature selection, dimensionality reduction, classification, and segmentation.

[29-33] presents different aspects of remote sensing, Spatio-temporal data, spectral data and other data processing and also novel aspects.

3. Methodology For 1d, 2d and 3d Cnn.

3.1. Data Description

Dataset	Salinas Data		
Parameters	Indian Pines	Pavia University	
Location	Indiana (USA)	Pavia, northern Italy	Salinas Valley, California
Data Type	Hyperspectral	Hyperspectral	Hyperspectral
Number Of Bands	220	115	224
Bands in Corrected Data	200	103	204

Total Classes	16,Wheat,Soybean-clean,Oats,Corn,Grass-etc.	9,Asphalt,Meadows,Gravel,Trees,,Bare Soil etc.	16,Brocoli_green_weeds_1, Grapes_untrained,Lettuce_omaine_4wk etc.
Spatial Resolution	20 m	1.3 m	3.7 m
Total No of Pixels	145*145=21025	610, 340=207400	512, 217=111104
File Format Used	.mat File	.mat File	.mat File

The Indian Pines scene was acquired by the AVIRIS sensor over the Indian Pines test site in North-western Indiana, encompassing 145 * 145 pixels and featuring 224 spectral reflectance bands. The Salinas scene was captured using the 224-band AVIRIS sensor over Salinas Valley, California, and is distinguished by its high spatial resolution with 3.7-meter pixels. The covered area spans 512 lines by 217 samples. Pavia University scenes

were obtained through the ROSIS sensor during a flight campaign over Pavia, northern Italy. Pavia University's dataset comprises 103 spectral bands, and the scene dimensions are 610 * 340 pixels[28].

Indian Pines contains images of a rural area in Indiana, USA, with 16 classes of crops and natural vegetation. It can be used to show how hyperspectral data can help identify different types of crops and monitor their health and growth. Pavia University contains images of an urban area in Pavia, Italy, with 9 classes of buildings and roads. It can be used to show how hyperspectral data can help distinguish different types of land cover and land use in urban environments. Salinas contains images of an agricultural area in Salinas Valley, California, USA, with 16 classes of crops and soil. It can be used to show how hyperspectral data can help detect and characterize different materials based on their spectral properties.

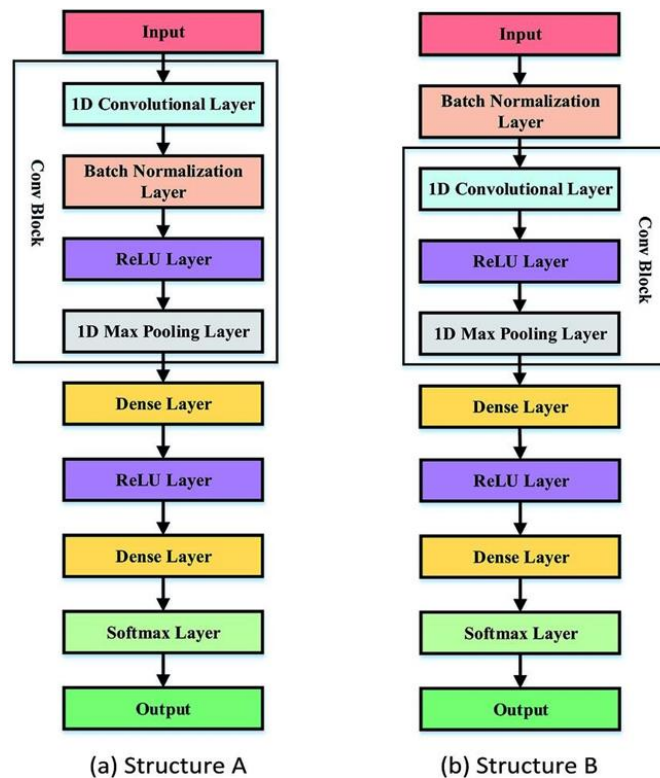


Fig 1.: Proposed Methodology

Data Reshaping for Convolutional Neural Networks (CNNs)

To prepare the data for analysis using 1D, 2D, and 3D CNNs, the following reshaping procedures were employed:

- For 1D CNN: Each pixel's spectral signature (200-dimensional vector) was extracted and treated as an

individual sample, leading to a reshaped dataset of dimensions (21025, 200), where 21025 represents the total number of spatial pixels.

- For 2D CNN: The dataset was interpreted as multi-channel 2D images, akin to RGB images in standard image processing, but with 200 spectral channels, retaining its original spatial dimensions (145, 145,

200).

- For 3D CNN: The data was used in its intrinsic 3D form (145, 145, 200), encapsulating both spatial and spectral information.

Normalization

Given the varying magnitudes of spectral reflectance values, normalization was a critical step to standardize the data. This involved scaling the dataset so that each spectral band had a mean of zero and a standard deviation of one. This step was essential to ensure that no single band disproportionately influenced the model due to its magnitude.

Train-Test Split

For model evaluation and to mitigate overfitting, the dataset was partitioned into training and testing subsets. A stratified split was performed to maintain the proportion of samples from each class in both subsets. Typically, 70% of the data was used for training, and the remaining 30% constituted the testing set.

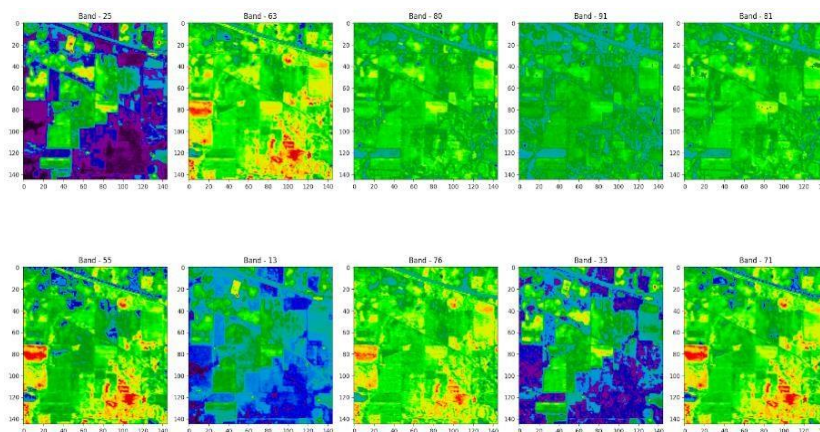


Fig 2.: Band Extraction

The dataset was restructured to cater to the requirements of different Convolutional Neural Network (CNN) architectures. For the 1D CNN, the data was reshaped into a vector form, treating each pixel's spectral signature as a separate instance. The 2D CNN architecture necessitated the retention of spatial information in a two-dimensional format, akin to traditional image data but with multiple spectral channels. Lastly, the 3D CNN utilized the data in its volumetric form, embracing both spatial and spectral dimensions.

3.2. Model Architectures

The study compared three distinct CNN architectures - 1D, 2D, and 3D - each tailored to the nature of the hyperspectral data.

1D Convolutional Neural Network (CNN): The 1D CNN was designed to analyze the spectral signatures linearly. It comprised an input layer accepting 200-dimensional vectors, followed by multiple convolutional layers with

Data Augmentation

To enhance the robustness of the models and to address issues of limited data in certain classes, data augmentation techniques such as spectral rotation and flipping were considered. This step was contingent on the initial model performance and data availability for each class.

One-Hot Encoding of Labels

For classification purposes, the ground truth labels were one-hot encoded. This process converted categorical labels into a binary matrix representation, suitable for the output layer of the CNN models.

Hyperparameter Tuning

In preparation for model optimization, a range of hyperparameters for each CNN type was defined. These included, but were not limited to, the number of filters, kernel size, density of fully connected layers, and dropout rates. Random search was employed to navigate through this hyperparameter space, balancing comprehensiveness and computational efficiency.

1D convolution operations. Pooling layers were interspersed to reduce dimensionality and computational load. The network concluded with fully connected layers and a softmax output layer for multi-class classification.

2D Convolutional Neural Network (CNN): The 2D CNN mimicked traditional image processing techniques, treating the hyperspectral data as multi-channel images. The model started with 2D convolutional layers that processed spatial features, followed by 2D pooling layers. The architecture culminated in fully connected layers, paralleling the structure of the 1D CNN but adapted for 2D input.

3D Convolutional Neural Network (CNN): The 3D CNN was the most comprehensive, processing the data in its original three-dimensional form. This architecture utilized 3D convolutional layers to simultaneously capture spatial and spectral features. Similar to its counterparts, it also featured pooling layers and fully connected layers, concluding with a softmax output layer.

3.3. Hyperparameter Tuning and Model Training

The hyperparameters for each model were optimized using a random search approach. This involved defining a range for key hyperparameters such as the number of filters, kernel size, number of dense units, and dropout rate. Models were trained using randomly selected combinations of these parameters, and their performance was assessed based on classification accuracy. The optimal set of parameters was then chosen for the final model training.

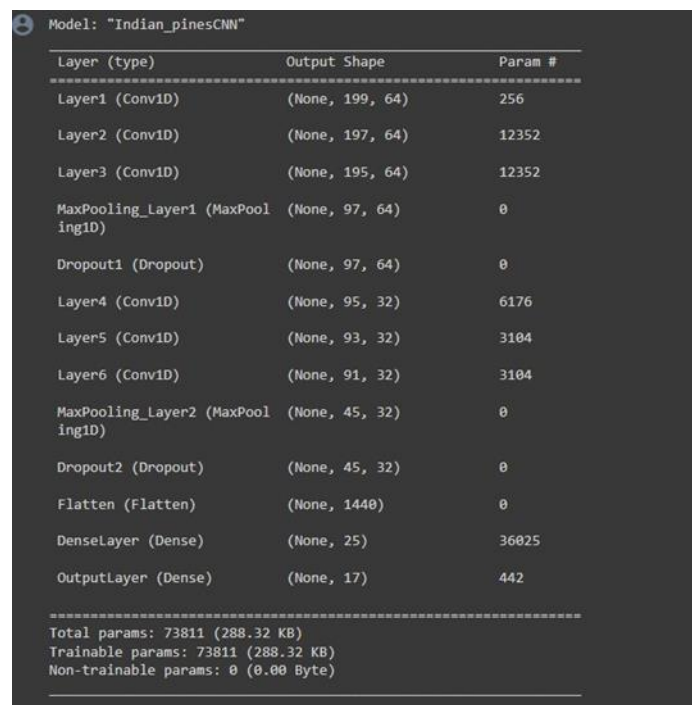
Each model was compiled using the Adam optimizer and categorical cross-entropy loss function, reflecting the multi-class nature of the dataset. The models were trained on the preprocessed dataset, with a portion of the data reserved for validation to monitor and mitigate overfitting.

3.4. Evaluation Metrics

The performance of the 1D, 2D, and 3D CNNs was evaluated using accuracy, precision, recall, and F1-score. These metrics provided a comprehensive view of each model's performance, considering aspects such as the balance between sensitivity and specificity, and the harmonic mean of precision and recall.

The 3 datasets will be used to train 3 different CNN Models. The CNN model for the Hyperspectral Data has 6 convolutional Layers, 2 Max Pooling Layers, 2 Dropouts, 1 Dense Layer with Relu and Output with Softmax.

The Architecture of the CNN model is as follows: -



Layer (type)	Output Shape	Param #
Layer1 (Conv1D)	(None, 199, 64)	256
Layer2 (Conv1D)	(None, 197, 64)	12352
Layer3 (Conv1D)	(None, 195, 64)	12352
MaxPooling_Layer1 (MaxPooling1D)	(None, 97, 64)	0
Dropout1 (Dropout)	(None, 97, 64)	0
Layer4 (Conv1D)	(None, 95, 32)	6176
Layer5 (Conv1D)	(None, 93, 32)	3184
Layer6 (Conv1D)	(None, 91, 32)	3184
MaxPooling_Layer2 (MaxPooling1D)	(None, 45, 32)	0
Dropout2 (Dropout)	(None, 45, 32)	0
Flatten (Flatten)	(None, 1440)	0
DenseLayer (Dense)	(None, 25)	36025
OutputLayer (Dense)	(None, 17)	442

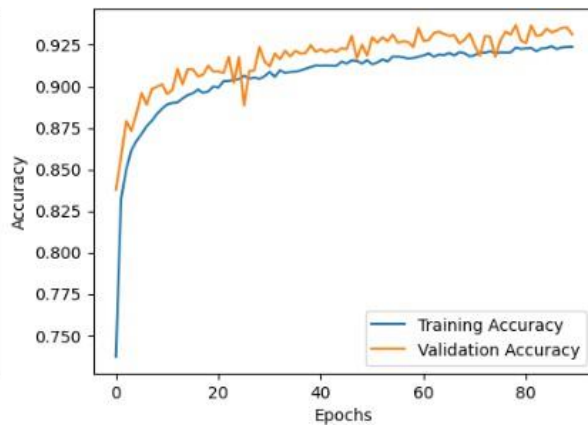
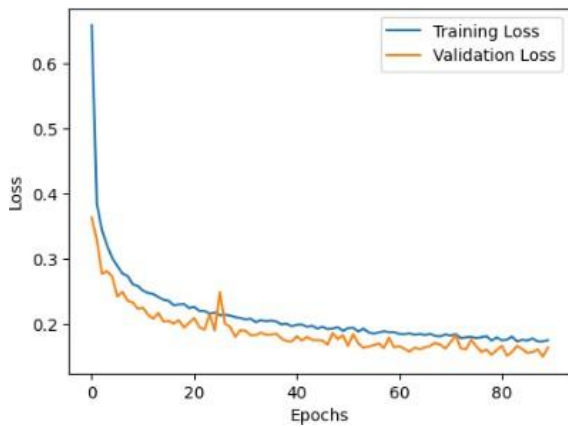
=====
Total params: 73811 (288.32 KB)
Trainable params: 73811 (288.32 KB)
Non-trainable params: 0 (0.00 Byte)

These CNN models will then be fused and put through an LSTM network with the intention of getting the required Output and Time series analysis of the data to compare the change in value in the region. The LSTM network will have 4 output values. High value, Good, Low, Very Low.

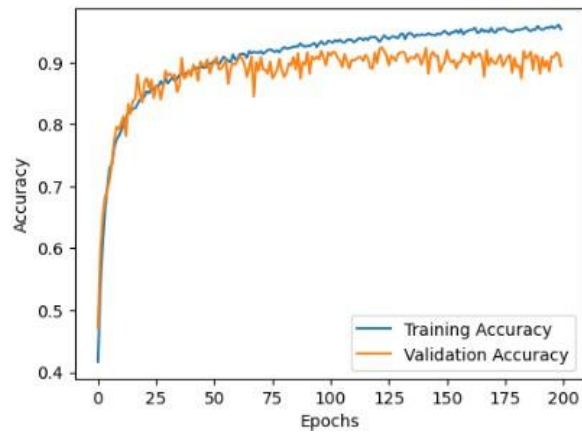
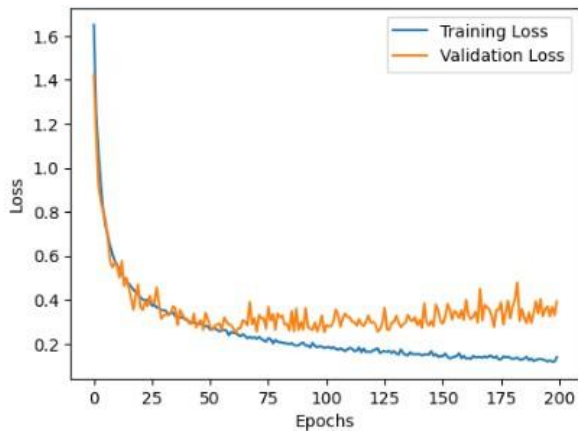
The output of the model will be plotted and Geo-referenced to create a Tiff file that can be used as a layer in GIS software. The Output of the model will be assigned to the respective area and using the Coordinates of the area the Tiff file will be created.

4. Results and Discussion

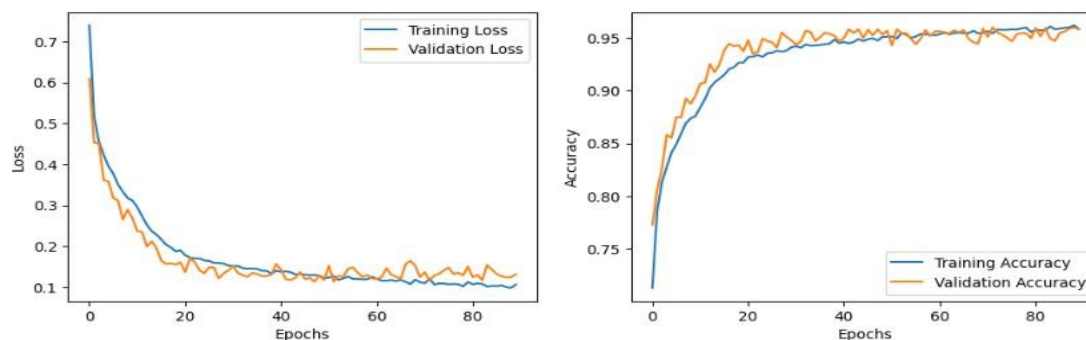
Evaluation Matrix	Accuracy	Precision	Recall
Datasets			
Salinas	CNN:0.9351	CNN:0.9353	CNN:0.9362
	RF:0.9491	RF:0.9568	RF:0.9409
	SVC:0.9192	SVC:0.9220	SVC:0.9169
Pavia	CNN:0.948	CNN:0.9489	CNN:0.9485
	RF:0.9124	RF:0.9397	RF:0.9194
	SVC:0.9221	SVC:0.9222	SVC:0.9225
Indian Pines	CNN :0.9102	CNN :0.9113	CNN:0.9103
	RF:0.7721	RF:0.9314	RF:0.7724
	SVC:0.8902	SVC:0.8952	SVC:0.8904



Results of Training of Salinas Dataset (1-D CNN)



Results of Training of Indian Pines Dataset (1-D CNN)



Results of Pavia Dataset (1-D CNN)

5. Conclusion

The Convolutional neural networks (CNNs) will be utilized in this study to build hyperspectral image categorization remote sensing technology. Achieving good generalization, addressing difficulties like overfitting, as well as improving classification accuracy were the objectives. In order to increase efficacy and reliability in hyperspectral image classification, the study compared 1-D CNN, 2-D CNN, Support Vector Classifier, Random Forest performance on benchmark datasets and built remote sensing technologies to close the gap between traditional methods and modern standards.

References:

- [1] Geospatial World. (2010). High Resolution Remote Sensing Sensors. [online] Available at: <https://www.geospatialworld.net/article/high-resolution-remote-sensing-sensors/>.
- [2] Shrestha, R. and Hardeberg, J.Y., 2014, November. Evaluation and comparison of multispectral imaging systems. In Color and Imaging Conference (Vol. 2014, No. 2014, pp. 107-112). Society for Imaging Science and Technology.
- [3] Yokoya, N., Grohnfeldt, C. and Chanussot, J., 2017. Hyperspectral and multispectral data fusion: A comparative review of the recent literature. *IEEE Geoscience and Remote Sensing Magazine*, 5(2), pp.29-56.
- [4] Abdurraheem, M.I., Zhang, W., Li, S., Moshayedi, A.J., Farooque, A.A. and Hu, J., 2023. Advancement of Remote Sensing for Soil Measurements and Applications: A Comprehensive Review. *Sustainability*, 15(21), p.15444.
- [5] Lv, W. and Wang, X., 2020. Overview of hyperspectral image classification. *Journal of Sensors*, 2020.
- [6] Stuart, M.B., McGonigle, A.J. and Willmott, J.R., 2019. Hyperspectral imaging in environmental monitoring: A review of recent developments and technological advances in compact field deployable systems. *Sensors*, 19(14), p.3071.
- [7] Shimoni, M., Haelterman, R. and Perneel, C., 2019. Hyperspectral imaging for military and security applications: Combining myriad processing and sensing techniques. *IEEE Geoscience and Remote Sensing Magazine*, 7(2), pp.101-117.
- [8] Adão, T., Hruška, J., Pádua, L., Bessa, J., Peres, E., Morais, R. and Sousa, J.J., 2017. Hyperspectral imaging: A review on UAV-based sensors, data processing and applications for agriculture and forestry. *Remote sensing*, 9(11), p.1110.
- [9] Cui, R., Yu, H., Xu, T., Xing, X., Cao, X., Yan, K. and Chen, J., 2022. Deep learning in medical hyperspectral images: A review. *Sensors*, 22(24), p.9790.
- [10] Makantasis, K., Karantzalos, K., Doulamis, A. and Doulamis, N., 2015, July. Deep supervised learning for hyperspectral data classification through convolutional neural networks. In 2015 IEEE international geoscience and remote sensing symposium (IGARSS) (pp. 4959-4962). IEEE.
- [11] Lee, H. and Kwon, H., 2017. Going deeper with contextual CNN for hyperspectral image classification. *IEEE Transactions on Image Processing*, 26(10), pp.4843-4855.
- [12] Bai, J., Ding, B., Xiao, Z., Jiao, L., Chen, H. and Regan, A.C., 2021. Hyperspectral image classification based on deep attention graph convolutional network. *IEEE Transactions on Geoscience and Remote Sensing*, 60, pp.1-16.
- [13] Gao, H., Chen, Z. and Li, C., 2021. Sandwich convolutional neural network for hyperspectral image classification using spectral feature enhancement. *IEEE Journal of Selected Topics in Applied Earth Observations and Remote Sensing*, 14, pp.3006-3015.
- [14] Ghaderizadeh, S., Abbasi-Moghadam, D., Sharifi, A., Zhao, N. and Tariq, A., 2021. Hyperspectral image classification using a hybrid 3D-2D convolutional neural networks. *IEEE Journal of Selected Topics in Applied Earth Observations and Remote Sensing*, 14, pp.7570-7588.

- [15] Song, W., Li, S., Fang, L. and Lu, T., 2018. Hyperspectral image classification with deep feature fusion network. *IEEE Transactions on Geoscience and Remote Sensing*, 56(6), pp.3173-3184.
- [16] Ahmad, M., Mazzara, M. and Distefano, S., 2021. Regularized CNN feature hierarchy for hyperspectral image classification. *Remote Sensing*, 13(12), p.2275.
- [17] He, X. and Chen, Y., 2019. Optimized input for CNN-based hyperspectral image classification using spatial transformer network. *IEEE Geoscience and Remote Sensing Letters*, 16(12), pp.1884-1888.
- [18] Ahmad, M., Shabbir, S., Raza, R.A., Mazzara, M., Distefano, S. and Khan, A.M., 2021. Hyperspectral image classification: Artifacts of dimension reduction on hybrid CNN. *arXiv preprint arXiv:2101.10532*.
- [19] Roy, S.K., Krishna, G., Dubey, S.R. and Chaudhuri, B.B., 2019. HybridSN: Exploring 3-D-2-D CNN feature hierarchy for hyperspectral image classification. *IEEE Geoscience and Remote Sensing Letters*, 17(2), pp.277-281.
- [20] Vaddi, R. and Manoharan, P., 2020. Hyperspectral image classification using CNN with spectral and spatial features integration. *Infrared Physics & Technology*, 107, p.103296.
- [21] Fan, X., Chen, L., Xu, X., Yan, C., Fan, J. and Li, X., 2023. Land Cover Classification of Remote Sensing Images Based on Hierarchical Convolutional Recurrent Neural Network. *Forests*, 14(9), p.1881.
- [22] Hong, D., Han, Z., Yao, J., Gao, L., Zhang, B., Plaza, A. and Chanussot, J., 2021. SpectralFormer: Rethinking hyperspectral image classification with transformers. *IEEE Transactions on Geoscience and Remote Sensing*, 60, pp.1- 15.
- [23] Li, S., Song, W., Fang, L., Chen, Y., Ghamisi, P. and Benediktsson, J.A., 2019. Deep learning for hyperspectral image classification: An overview. *IEEE Transactions on Geoscience and Remote Sensing*, 57(9), pp.6690-6709.
- [24] Qing, C., Ruan, J., Xu, X., Ren, J. and Zabalza, J., 2019. Spatial-spectral classification of hyperspectral images: a deep learning framework with Markov Random fields based modelling. *IET Image Processing*, 13(2), pp.235-245.
- [25] Gao, Q., Lim, S. and Jia, X., 2018. Hyperspectral image classification using convolutional neural networks and multiple feature learning. *Remote Sensing*, 10(2), p.299.
- [26] Chen, Y., Jiang, H., Li, C., Jia, X. and Ghamisi, P., 2016. Deep feature extraction and classification of hyperspectral images based on convolutional neural networks. *IEEE transactions on geoscience and remote sensing*, 54(10), pp.6232-6251.
- [27] Petersson, H., Gustafsson, D. and Bergstrom, D., 2016, December. Hyperspectral image analysis using deep learning—A review. In 2016 sixth international conference on image processing theory, tools and applications (IPTA) (pp. 1-6). IEEE.
- [28] www.ehu.eus. (n.d.). Hyperspectral Remote Sensing Scenes - Grupo de Inteligencia Computacional (GIC). [online] Available at: https://www.ehu.eus/ccwintco/index.php/Hyperspectral_Remote_Sensing_Scenes.
- [29] A. Abdollahi, B. Pradhan, S. Gite and A. Alamri, "Building Footprint Extraction from High Resolution Aerial Images Using Generative Adversarial Network (GAN) Architecture," in *IEEE Access*, vol. 8, pp. 209517-209527, 2020, doi: 10.1109/ACCESS.2020.3038225.
- [30] Abdollahi, A., Pradhan, B., Gite, S., & Alamri, A. (2020). Building footprint extraction from high resolution aerial images using generative adversarial network (GAN) architecture. *IEEE Access*, 8, 209517-209527.
- [31] Joshi, A.; Pradhan, B.; Gite, S.; Chakraborty, S. Remote-Sensing Data and Deep-Learning Techniques in Crop Mapping and Yield Prediction: A Systematic Review. *Remote Sens.* **2023**, *15*, 2014. <https://doi.org/10.3390/rs15082014>
- [32] Serbouti, I.; Raji, M.; Hakdaoui, M.; El Kamel, F.; Pradhan, B.; Gite, S.; Alamri, A.; Maulud, K.N.A.; Dikshit, A. Improved Lithological Map of Large Complex Semi-Arid Regions Using Spectral and Textural Datasets within Google Earth Engine and Fused Machine Learning Multi-Classifiers. *Remote Sens.* **2022**, *14*, 5498. <https://doi.org/10.3390/rs14215498>
- [33] S. Gite, B. Pradhan, A. Alamri and K. Kotecha, "ADMT: Advanced Driver's Movement Tracking System Using Spatio-Temporal Interest Points and Maneuver Anticipation Using Deep Neural Networks," in *IEEE Access*, vol. 9, pp. 99312-99326, 2021, doi: 10.1109/ACCESS.2021.3096032.